EXAFS determination of cation local order in layered perovskites

M.E. Montero-Cabrera[a], M. García-Guaderrama[b], A. Mehta[c], S. Webb[c], L. Fuentes-Montero[a], J.A. Duarte Moller[a], and L. Fuentes-Cobas[a]

[a] *Centro de Investigación en Materiales Avanzados, Chihuahua, México.*
[b] *Universidad Nacional Autónoma de México, México, D.F.*
[c] *Stanford Synchrotron Radiation Laboratory, CA, USA.*

Recibido el 14 de mayo de 2007; aceptado el 26 de octubre de 2007

EXAFS analysis of $Bi_6Ti_3Fe_2O_{18}$ Aurivillius ceramic was performed to elucidate the local environment of Fe cations. Experiments were performed at Stanford Synchrotron Radiation Laboratory, at T = 10, 30, 50, 75, 100 and 298 K, in fluorescence regime. EXAFS spectra were processed using the ab initio multiple scattering program FEFF6. Distances among representative atomic pairs were refined. As a basic result, the previous hypothesis suggested by X-ray diffraction experiments, regarding a preference of iron atoms for the centered perovskite layer of the unit cell, was confirmed.

Keywords: synchrotron radiation; EXAFS; Aurivillius ceramic; local order.

Se determinó por EXAFS el entorno local de los cationes de hierro en la cerámica Aurivillius $Bi_6Ti_3Fe_2O_{18}$. La parte experimental de la investigación se realizó en el Laboratorio de Radiación Sincrotrónica de Stanford, en régimen de fluorescencia, a temperaturas de 10, 30, 50, 75, 100 y 298 K. Los espectros EXAFS fueron procesados mediante el software ab initio para dispersión múltiple FEFF6. Se refinaron las distancias inter-atómicas de pares representativos. Un resultado básico del trabajo es la confirmación de la hipótesis, sugerida por resultados de difracción de rayos x, relativa a la preferencia de los átomos de hierro por ocupar posiciones en la capa perovskita del nivel central en la celda unitaria.

Descriptores: radiación sincrotrónica; EXAFS; cerámica de Aurivillius; orden local.

PACS: 61.10.Ht; 77.84.-s

1. Introduction

Magnetoelectric multiferroics are one of the most exciting materials' families investigated today [1]. Coexistence of magnetic and electric order is hard to achieve, but remarkably useful. Perovskite and perovskite-related crystal structures show themselves today as the most promising candidates for exhibiting multiferroic nature. Iron-containing Aurivillius phases [2] are ferroelectric layered perovskites that, in principle, are capable of being also ferromagnetic. A necessary condition for magnetic order is the existence of structural ordering of iron cations among selected crystallographic sites. $Bi_6Ti_3Fe_2O_{18}$ is a hard to synthesize, but particularly interesting 5-layered Aurivillius phase. A recent synchrotron diffraction study [3] suggests that –on a long range scale- the iron cations are preferentially ordered in the "equatorial" perovskite layer. Confirming this possibility would lead to a favorable scenario for super-exchange interactions among iron cations and the manifestation of some kind of magnetic ordering. Testing this hypothesis at local level is the objective of the present work.

2. Resume about extended X-ray absorption fine structure

Extended X-ray absorption fine structure (EXAFS) spectroscopy refers to the oscillatory dependence of X-ray absorption coefficient. In recent times, it has become a useful tool for investigating short range order in crystals and molecular interactions. Experimentally, it involves the measurement of the X-ray absorption coefficient as a function of photon energy above an X-ray absorption K or L edges of a probe atom [4, 5]. These experiments require tuned synchrotron radiation. The absorption edge energies used for EXAFS are in the range of 4 to 40 keV.

X-ray absorption involves the excitation of a core electron into a final state above the top occupied electronic state of a specific atom present in the material. The excited electron is referred to as a photoelectron and its final state is composed of an outgoing electronic wave function and many singly and multiply reflected electronic waves.

The EXAFS spectrum $\chi(E)$ is defined phenomenologically [6] as the normalized, oscillatory part of the x-ray absorption coefficient above a given absorption edge, i.e.,

$$\chi(E) = [\mu(E) - \mu_0(E)]/\Delta\mu_0, \qquad (1)$$

where $\mu_0(E)$ is the smoothly varying background absorption from the "bare" atom (including contributions, if any, from other edges) and $\Delta\mu_0$ is a normalization factor that arises from the net increase in the total atomic background absorption at the edge in question.

After the work of Sayers, Stern and Lytle [4] it was widely recognized that EXAFS function $\chi(E)$ provides information about the local structure around the absorbing atom. In most experiments, data up to the fourth nearest neighbors may be obtained, even further out in exceptional cases. Obtainable information includes coordination numbers, near neighbor distances, mean squared relative dis-

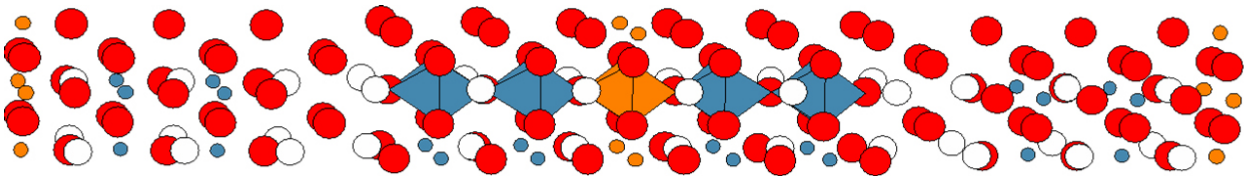

FIGURE 1. The crystal structure of $Bi_6Ti_3Fe_2O_{18}$ [ref 3]. Space group: Fmm2. Spheres: large red → O; small blue/orange → Ti/Fe; large white → Bi. a = 49.342 Å; b = 5.4655 Å; c = 5.4967 Å. Polar axis c points roughly outwards from the figure.

placements (Debye-Waller factor) and, in some cases, bond angles. The information is averaged over all absorbing atoms of the same type. In EXAFS, the measurement of each absorption edge is done almost always separately, providing the structure around different types of probes. This includes low concentration elements of the order of 1%.

At present, EXAFS experimental data $\chi(E)$ are analyzed by refining the theoretically calculated EXAFS spectrum of model structures about the core atom [7–9]. For this analysis, is customized to transform spectra to the k (wave number) space and to make the Fourier Transform of that spectra. Experimental results of EXAFS distances have less significant digits than those obtained from high resolution X-Ray Diffraction in crystalline systems. On the other hand, EXAFS gives local information and may differentiate between static and thermal contributions to Debye-Waller factors.

3. Experiment

Sample was obtained by molten salts synthesis, according to the description given by García-Guaderrama et al [3]. The structure obtained by synchrotron radiation diffraction and reported in the cited reference is shown in Figure 1. $Bi_6Ti_3Fe_2O_{18}$ crystals show a layered structure, with five perovskite octahedra "sandwiched" between bismuth oxide sheets. Small (Ti/Fe) cations occupy virtually the centers of the shown perovskite octahedra. Diffraction data suggest that Fe cations show a tendency to be located at the central octahedra, far from the Bi-oxide layers. In this context, the information obtainable by means EXAFS is highly valuable.

EXAFS spectra of $Bi_6Ti_3Fe_2O_{18}$ at 10, 30, 50, 75, 100 y 298 K were measured. Fe K absorption edge spectra (about 7112 eV) were obtained at SSRL beamline 2-3 using a Lytle fluorescence detector, at the mentioned temperatures. Raw data were processed with *SixPACK* package [10]. In the edge zone the energy intervals were ΔE = 0.35 eV. After 7114 eV, in the EXAFS zone, energy intervals corresponded to Δk = 0.04 Å^{-1}. Spectra were measured up to k = 11.7 Å^{-1}. Figure 2 presents the χ(k) spectra for T= 10 and 298 K.

4. Results and discussion

Figure 3 shows the amplitudes of the Fourier transform spectra χ(R) for all temperatures. This figure is related with the atomic radial distribution, centered at the x-ray absorbing atom (Fe) and somewhat shifted to the left. The near neighborhood of a Fe core atom is represented in Figure 4.

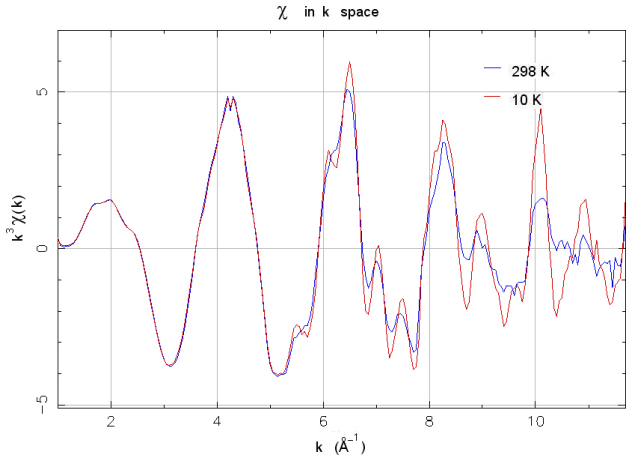

FIGURE 2. EXAFS spectra in wave number space of $Bi_6Ti_3Fe_2O_{18}$ sample for T=10 and 298K.

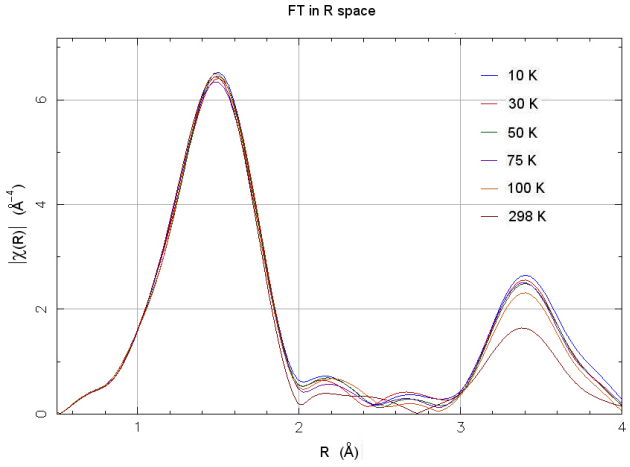

FIGURE 3. Fourier transforms of all spectra.

The first maxima of the χ(R) spectra occur at R $\approx$ 1.5 Å. They correspond (with a left shift of $\sim$ 0.4 Å) to the first Fe-O interatomic distances around the Fe core. These peaks are the superposition of signals associated with the various distances in the first Fe-O coordination shells (Fe-O^A, Fe-O^B) along the crystal volume. Partly due to disorder, partly due to practical limitations, the present EXAFS experiment did not resolve individual distances. In the broad temperature interval from 10 to 298 K the considered maximum appears almost unaltered.

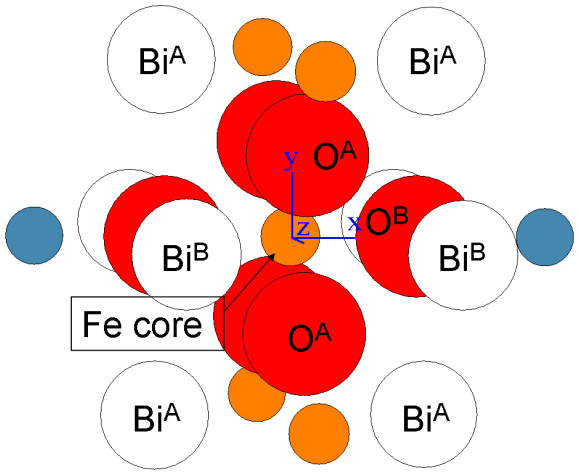

FIGURE 4. Closest neighbors to a Fe atom in $Bi_6Ti_3Fe_2O_{18}$.

The second maxima of the χ(R) spectra characterize the different Fe-Bi bonds. Interestingly, the effect of temperature is now significant. The 298 K second peak shows less intensity than the others. It is also somewhat broader. The origin of this feature is related with high values of Debye-Waller (DW) factors, as will be considered below.

EXAFS spectra were quantitatively processed using *Six-PACK* interface for *IFFEFIT* [11]. X-ray absorption was modeled by *FEFF6* [12], introducing in subroutine *ATOMS* the structure obtained by XRD. The distances among the Fe (core) and surrounding atoms were modeled. This includes Fe-bismuth, Fe-octahedral oxygen and Fe-closest Ti and Fe, in all possible positions. Six different configurations for two Fe atoms in the 5 perovskite layers were tried. Representing Ti as T and Fe as F, these configurations are: TTFFT, TTFTF, TTTFF, TFTTF, TFTFT and FTTTF. Fe core was selected, when possible, the closest to the center. For configurations TTFTF and TTFFT, when Fe cation is in the center, there are only three equations for fitting the Fe-Bi distance. For the rest of configurations there are six equations (one for each Bi). Only single scattering paths were considered. For the configurations TTFTF and TTFFT, 8 parameters were adjusted in the harmonic model and 14 parameters in the anharmonic. For configurations with Fe core farther from the cell center, 14 parameters were fitted in the harmonic model. The anharmonic model is impossible to be fitted, because there are more parameters than the number of independent points.

All configurations were processed for the six temperatures. Reduced $\Delta\chi^2$ values of less than 100 were obtained for configurations TTFFT and TTFTF at all temperatures. This range of $\Delta\chi^2$ values is not rare in EXAFS. Values of cation distances (R), Debye-Waller factors (σ^2) and anharmonic parameters (σ^3), corresponding to T = 10 and 298K, are shown in Table I. Figure 5 shows observed and calculated χ(R) for the TTFFT configuration.

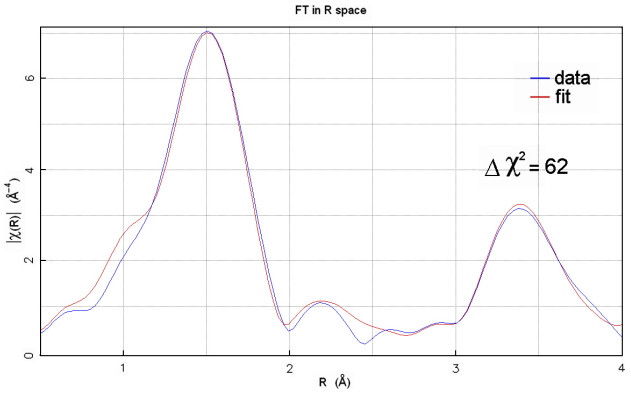

FIGURE 5. EXAFS function χ(R) obtained at T=10 K and fitting for configuration TTFFT.

TABLE I. EXAFS parameters for pairs of atoms obtained after fitting in cases of centered configurations for T=10 and 298 K. Uncertainties, in parenthesis, have the meaning of standards deviations.

Interatomic	EXAFS	T = 10 K		T= 298 K	
distances	Parameter	TTFFT	TTFTF	TTFFT	TTFTF
Fe-O^A	R (Å)	1.85 (4)	1.86 (8)	1.84 (4)	1.85 (5)
XRD=1.94 (Å)	σ^2(Å^2)	0.016 (2)	0.020 (4)	0.017 (2)	0.021 (3)
	σ^3(Å^3)	-0.003 (1)	-0.003 (4)	-0.003 (1)	-0.003 (2)
Fe-O^B	R (Å)	1.97 (4)	1.95 (8)	1.97 (3)	1.96 (4)
XRD=1.97 (Å)	σ^2(Å^2)	0.007 (2)	0.005 (2)	0.006 (1)	0.005 (1)
	σ^3(Å^3)	0.0005 (7)	- 0.0002 (10)	0.0003 (3)	0.00002 (2)
Fe-Bi^A	R (Å)	3.45 (2)	3.457 (6)	3.449 (3)	3.457 (6)
XRD=3.456 (Å)	σ^2(Å^2)	0.017 (5)	0.018 (5)	0.018 (7)	0.017 (4)
	σ^3(Å^3)	0.0150 (8)	0.015 (1)	0.015 (2)	0.015 (1)
Fe-Bi^B	R (Å)	3.56 (4)	3.67 (6)	3.54 (5)	3.67 (6)
XRD=3.65 (Å)	σ^2(Å^2)	0.004 (1)	0.004 (2)	0.006 (1)	0.008 (2)
	σ^3(Å^3)	0.0002 (5)	0.002 (1)	0.0003 (3)	0.002 (1)

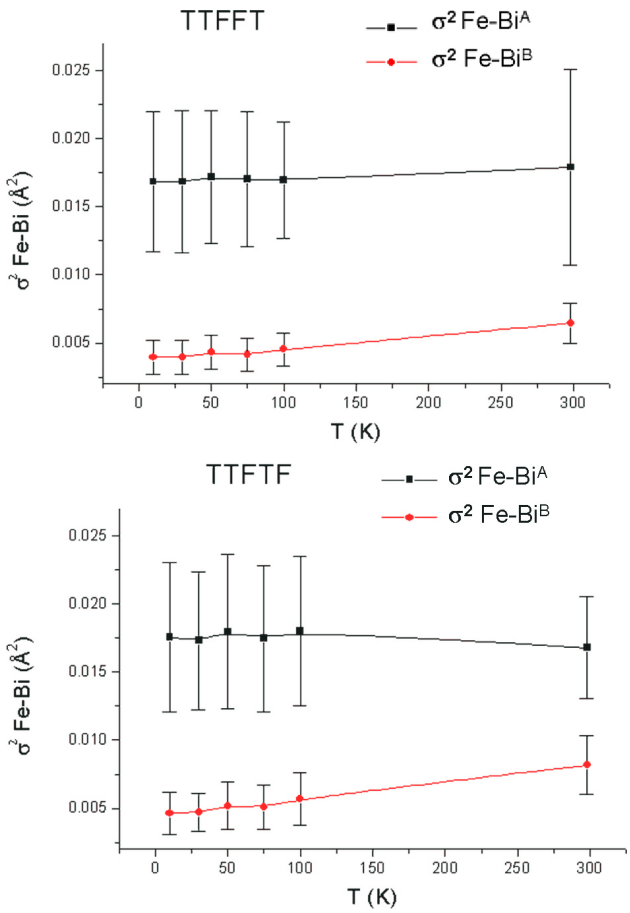

FIGURE 6. Debye-Waller factors of (Fe_{core}-Bi) pairs in perovskite layers, obtained by fitting spectra for all temperatures. TTFFT and TTFTF configurations.

Figure 6 presents the trend of DW factors for Fe core - Bi distances, as obtained in the fitting for centered configurations at all temperatures.

DW factors (σ^2) and anharmonic terms (σ^3) are consistently small for interactions of the type Fe-O^B and Fe-Bi^B that take place in the (xz) plane of the unit cell. Reasonably, these small DW factors are mostly thermo-vibrational in nature. A harmonic-vibrational model [13], applied to the DW results in the TTFFT configuration (for T = 10 and 298 K) is congruent with the consideration that Fe-Bi^B bonds are weaker than Fe-O^B, as is the case. The virtual absence of a static contribution to the DW factor associated with atoms in the xz plane is an indicator of a correlation among the static displacements of the atoms in that plane [6].

The observed large DW factors associated to the remaining atoms are not surprising. They were expected in view of the aspect of the 298 K Fe-Bi peak in the χ(R) plot (Figure 3). Low amplitude peaks appear as a consequence of large disorders and anharmonic vibrations that give rise to low-k contributions in the χ(k) spectrum [13].

For configurations with Fe farther from the center of the cell, in the frame of the harmonic model, reduced $\Delta\chi^2$ values are greater than 200. In some configurations uncertainties of Debye Waller factors diverge. This is a result of the asymmetry of the configuration, which severely affects the fitting. As general balance of the performed calculations, the central Fe model leads to an acceptable agreement among observed and calculated spectra. All other models lead to unacceptable observed-calculated relationships. This global result is the EXAFS argument that supports the central Fe-model.

Acknowledgements

Portions of this research were carried out at the Stanford Synchrotron Radiation Laboratory, a national user facility operated by Stanford University on behalf of the U.S. Department of Energy, Office of Basic Energy Sciences. The SSRL Structural Molecular Biology Program is supported by the Department of Energy, Office of Biological and Environmental Research, and by the National Institutes of Health, National Center for Research Resources, Biomedical Technology Program. Support from Consejo Nacional de Ciencia y Tecnología, CONACYT (Projects 42361 and 46515), is gratefully acknowledged.

1. N. Spaldin, *Nature Materials* **6** (2007) 1.
2. L. Fuentes, M. García, D. Bueno, M.E. Fuentes, and A. Muñoz, *Ferroelectrics* **336** (2006) 81.
3. M. García-Guaderrama, L. Fuentes-Montero, A. Rodriguez, and L. Fuentes, *Integrated Ferroelectrics* **83** (2006) 41.
4. D.E. Sayers, E.A. Stern, F.W. Lytle, *Phys Rev Lett.* **27** (1971) 1204.
5. E.A. Stern, "Heald SM. Basic principles and applications of EXAFS" *Handbook on synchrotron radiation* **2** (Amsterdam: North Holland, 1983) 955.
6. J.J. Rehr and R.C. Albers, *Review of Modern Physics*, **73** (2000) 621.
7. S.J. Gurman, N. Binsted, and I. Ross, *J Phys C* **19** (1986) 1845.
8. A. Filipponi, C.A. Di, and CR. Natoli, *Phys Rev B* **52** (1995) 15122.
9. A. Ankudinov, B. Ravel, J.J. Rehr, and S.D. Conradson, *Phys. Rev. B* **58** (1998) 7565.
10. S. Webb, http://www-ssrl.slac.stanford.edu/∼swebb/sixpack.htm
11. M. Newville, *J. Synchrotron Rad.* **8** (2001) 322.
12. SI Zabinsky, A. Ankudinov, R.C. Albers, M.J. and Eller, *Phys Rev B* **52** (1995) 2995.
13. B.K. Teo, *EXAFS: Basic Principles and Data Analysis* (Springer, Berlin, 1986).